Cell Reports, Volume *43*

Supplemental information

Functional genomics identifies *N*-acetyllactosamine extension of complex *N*-glycans as a mechanism to evade lysis by natural killer cells

Xiaoxuan Zhuang, James Woods, Yanlong Ji, Sebastian Scheich, Fei Mo, Sumati Rajagopalan, Zana A. Coulibaly, Matthias Voss, Henning Urlaub, Louis M. Staudt, Kuan-Ting Pan, and Eric O. Long

Supplemental Figures

Figure S1

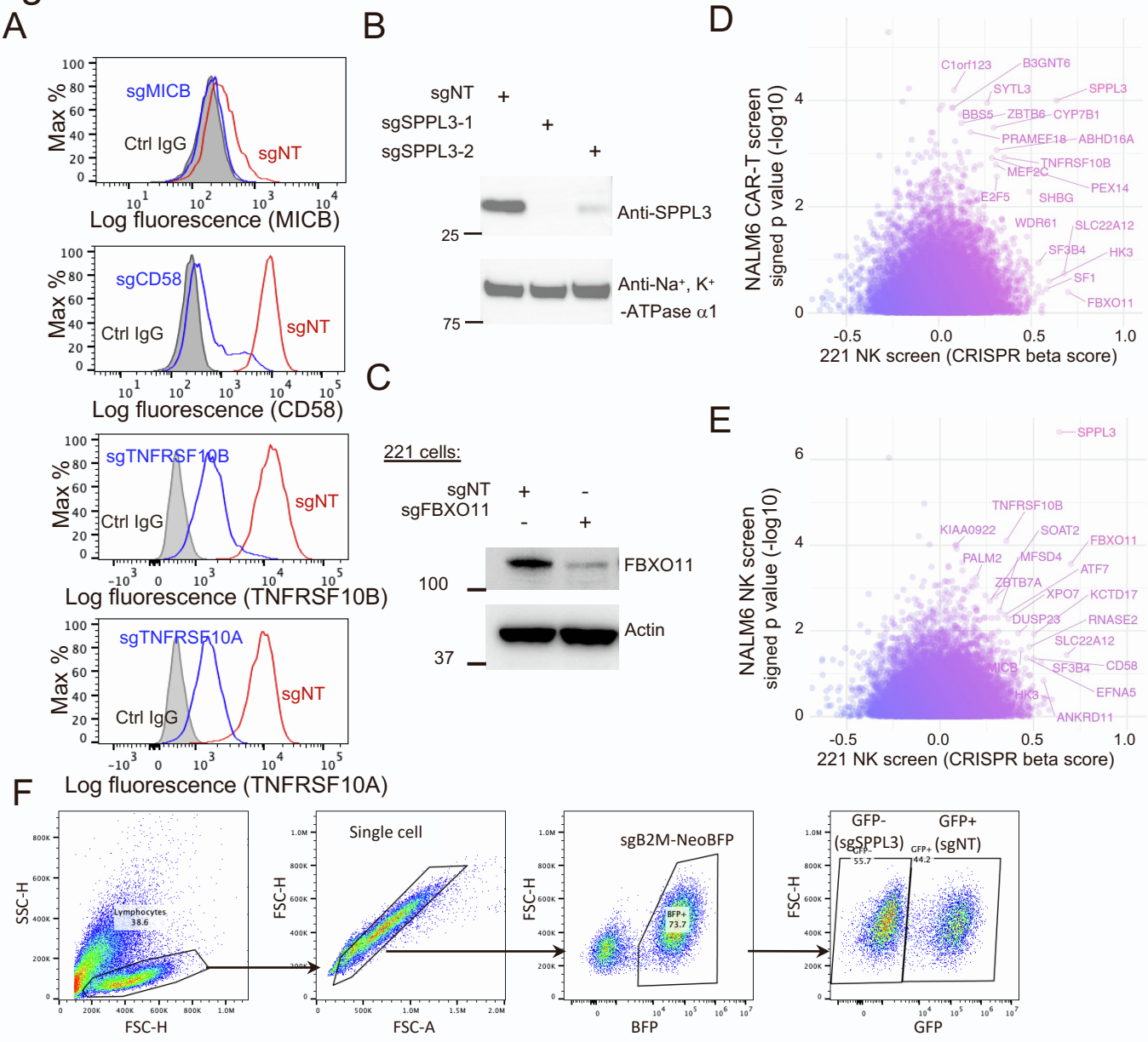

Fig. S1. Knockout efficiency of top hits in this screen, comparison of this screen to other screens and gating strategy for DLBCL cells killing assays, related to Figure 2. (A) Representative histograms showing staining of the indicated ligands of NK cell receptors on 221 cells expressing sgNT or sgRNAs targeting the respective ligands. (B) Immunoblot of SPPL3 isolated from the purified membrane fraction of 221 cells that expressed sgNT or sgSPPL3. Immunoblot of the Na^+, K^+-ATPase was used as loading control. (C) Immunoblot of FBXO11 from a lysate of 221 cells expressing sgNT or sgFBXO11. Immunoblot of actin was used as loading control. (D) Scatter plot show CRISPR beta score from 221 NK screen (x axis) comparing to signed p value from NALM6 CAR-T screen. (E) Scatter plot show CRISPR beta score from 221 NK screen (x axis) comparing to signed p value from NALM6 NK screen. (F) Gating strategy of flow cytometry-based killing assay using activated NK cells and DLBCL cell lines expressing sgSPPL3(GFP^-) or sgNT (GFP^+). Additionally, these cells express sgB2M (NeoBFP) to decrease MHC I expression and increase sensitivity to NK cells.

Figure S2

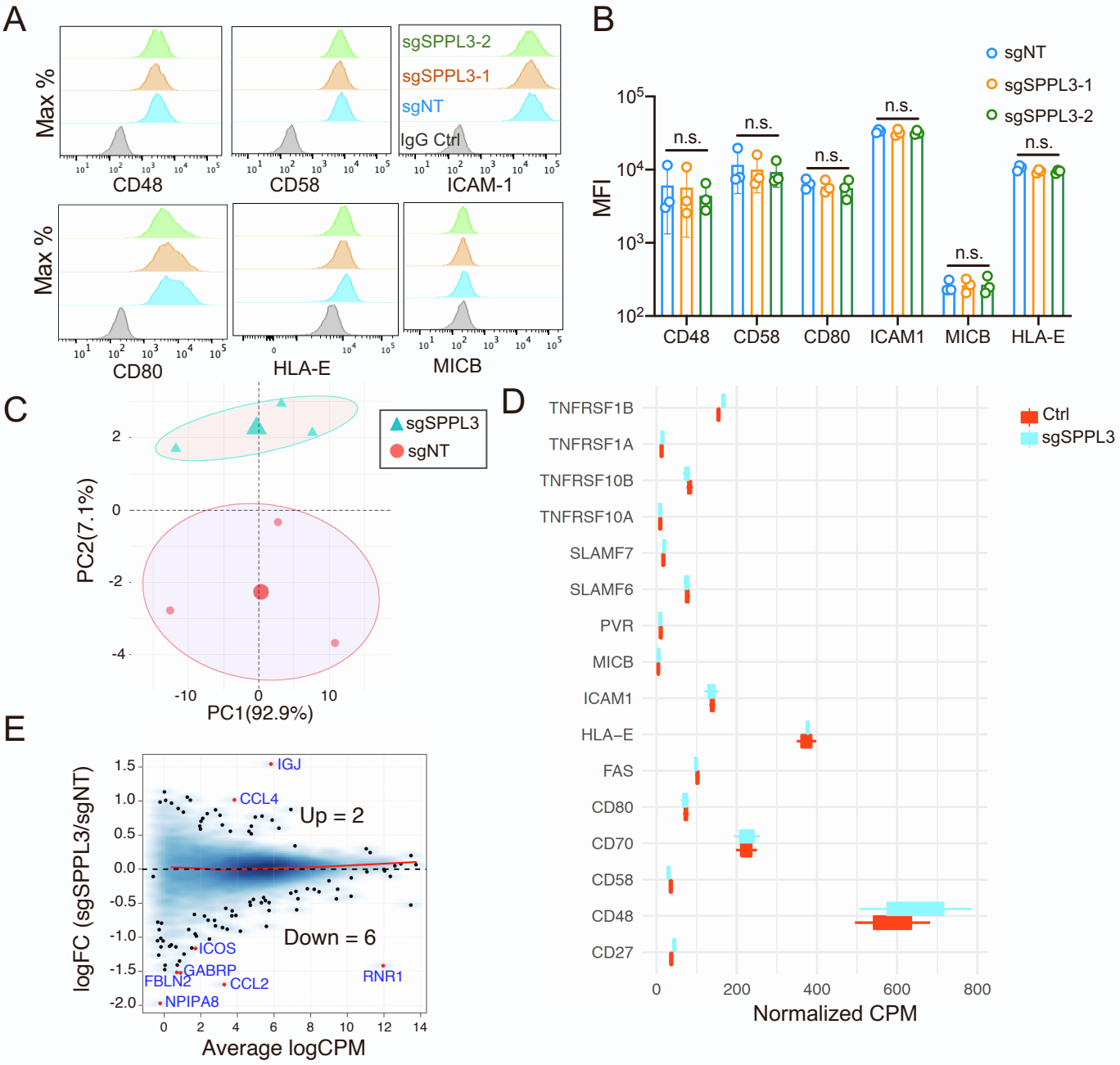

Fig. S2. Impact of *SPPL3* deletion on surface expression of ligands for NK receptors and their transcription. (A) Representative histograms showing surface staining of indicated ligands for NK receptors on 221 cells expressing sgNT or sgRNAs targeting *SPPL3*. (B) Statistics of mean fluorescence intensity (MFI) from 3 experiments carried out as in (A). Data shown as mean ± SEM (n=3, one-way ANOVA test, n.s. not significant). (C) PCA plot drawn with 95% confidence ellipses show sample clustering of RNA-seq data from sgNT and sgSPPL3 221 cells. (D) Transcription level of the indicated genes encoding ligands of NK receptors in sgNT and sgSPPL3 221 cells. (E) Mean-difference (MD) plot of global transcriptomic changes in sgSPPL3 221 cells compared to sgNT cells. Significantly differentially expressed genes were identified at an FDR of less than 5% (red dots and labels).

Figure S3

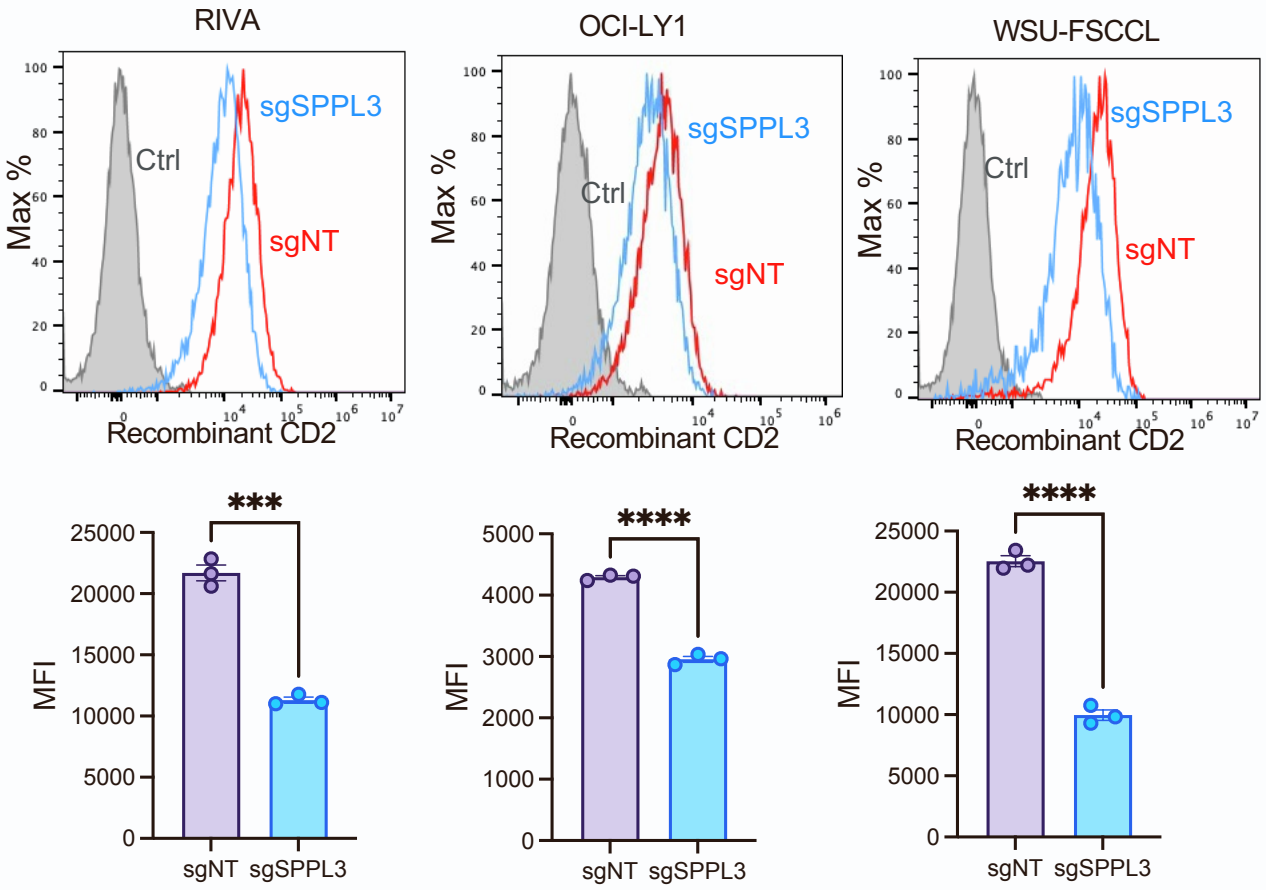

Fig. S3. Binding of recombinant CD2 to DLBCL cell lines. Representative histograms (upper panel) and statistic bar graphs (lower panel) show binding of soluble recombinant CD2 to the indicated DLBCL cell lines transfected with sgNT (red) or sgSPPL3 (blue). Ctrl represents staining using a recombinant human IgG1 Fc (gray). n=3, unpaired t-test, ****$p < 0.0001$, ***$p < 0.001$.

Figure S4

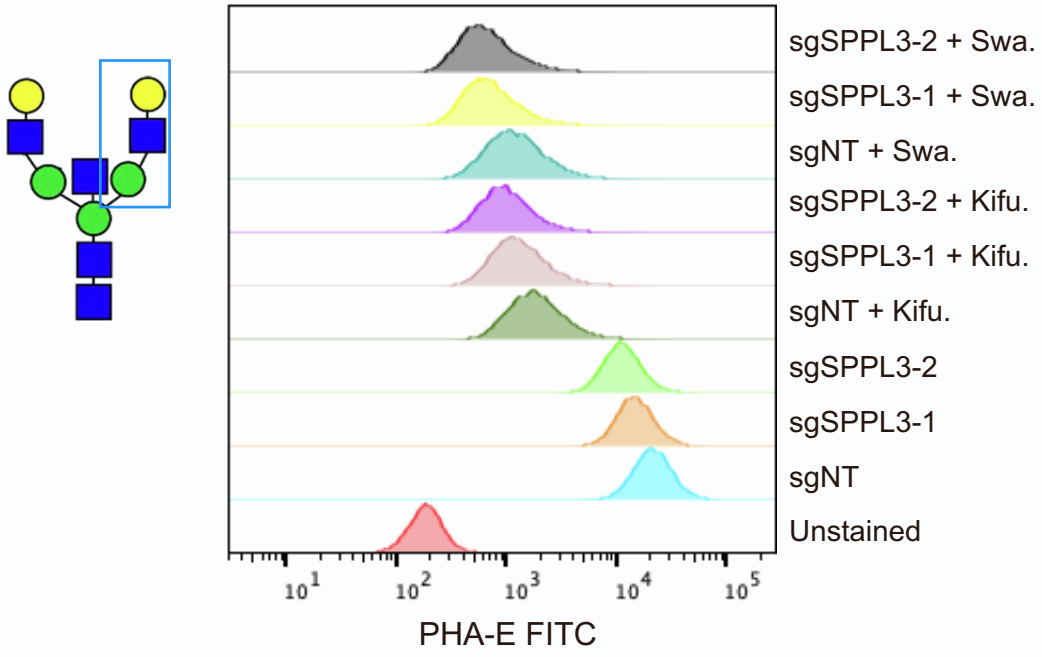

Fig. S4. Binding of PHA-E to 221 cells. Representative histograms of PHA-E staining of 221 cells expressing sgNT or sgRNAs targeting SPPL3. Cells were non-treated, treated with kifunensine (Kifu.) or swainsonine (Swa.).

Figure S5

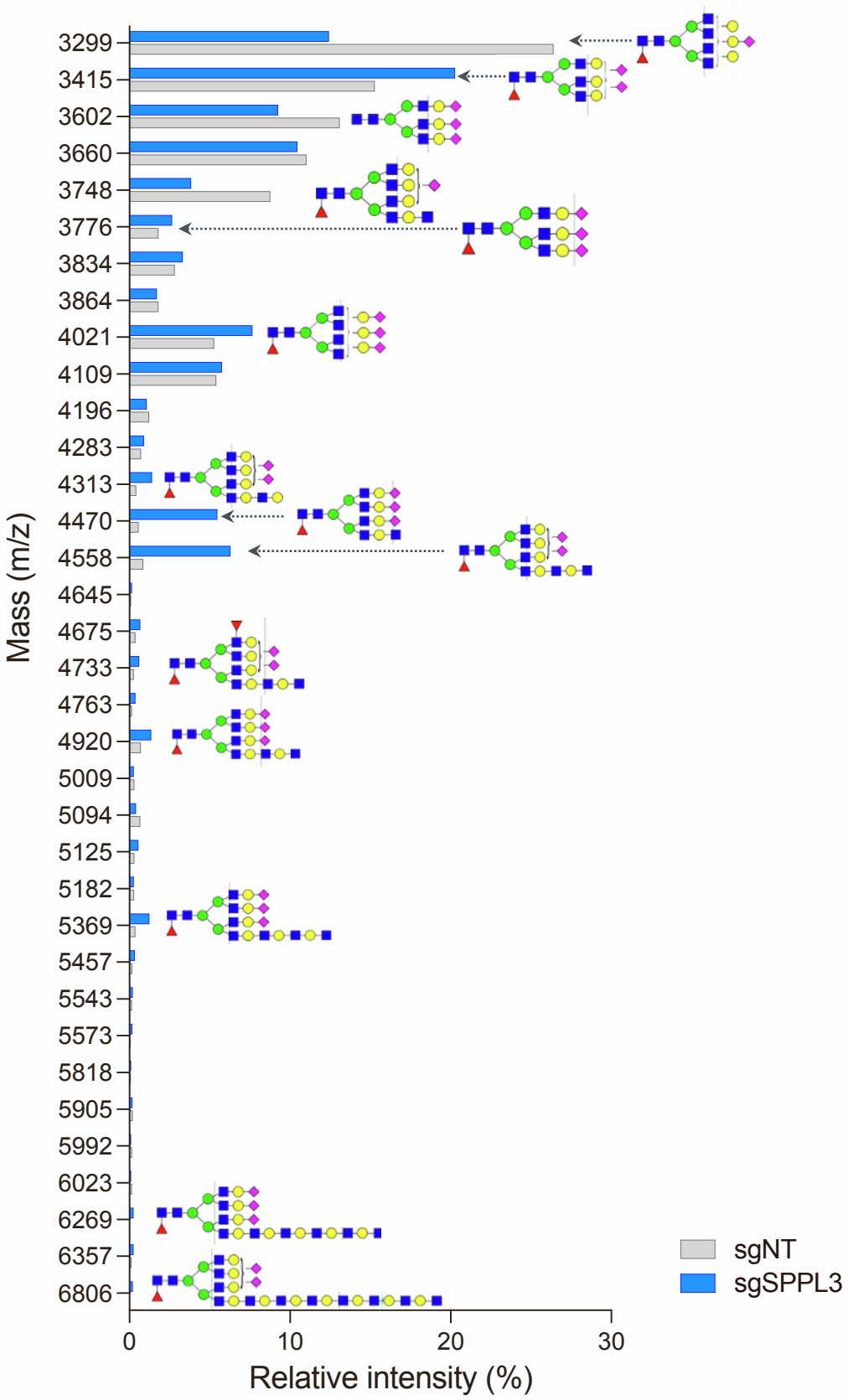
Mass (m/z)
3299
3415
3602
3660
3748
3776
3834
3864
4021
4109
4196
4283
4313
4470
4558
4645
4675
4733
4763
4920
5009
5094
5125
5182
5369
5457
5543
5573
5818
5905
5992
6023
6269
6357
6806
0
10
20
30
Relative intensity (%)
sgNT
sgSPPL3

Fig. S5. Glycomic analysis of high mass N-glycans on 221 cells expressing sgNT (grey) or sgSPPL3 (blue). Displayed are high mass N-glycans (>3298) detected in sgSPPL3-221 cells and compared with their abundance in sgNT-221 cells. All of them are at least tri-antennary. The two glycan forms that were reduced the most in sgSPPL3-221 cells are tetra-antennary forms with 2 unmodified Gal, neither sialylated nor extended with GlcNAc (m/z 3299 and 3748). The most enriched form was tetra-antennary with 3 sialylated Gal and 1 GlcNAc-elongated Gal (m/z 4470). Addition of Gal onto GlcNAc by a B4GALT generates LacNAc. The first tri-sialylated N-glycan with a LacNAc extension is at m/z 4920. This form has already acquired a GlcNAc on top of the first LacNAc. Further LacNAc elongations were detected as enriched N-glycans carrying 2 LacNAc (m/z 5369) and a low abundance 4 LacNAc (m/z 6269). The second most enriched (m/z 4558) has only 2 sialylated Gal, a LacNAc elongation, and a terminal GlcNAc. This terminal GlcNAc could be either on a separate branch or at the tip of the elongated branch, as depicted. This N-glycan could the precursor of the very large but low abundance N-glycan elongated with 6 LacNAc (m/z 6806). Note that the 6 LacNAc extensions could be distributed among the two unsialylated Gal. Note that the first glycan form carrying a LacNAc extension is at m/z 4313, which has two sialylated Gal, one free Gal and one LacNAc. It is a precursor of m/z 4558. It is formally possible that the terminal GlcNAc found on several N-glycan forms was added at an earlier step to the first mannose by MGAT3 (referred to as a bisection). It is however unlikely because bisection inhibits further branching by MGAT4 and MGAT5.